Wearable Technologies (2024), 5, e19
doi:10.1017/wtc.2024.22

CAMBRIDGE UNIVERSITY PRESS

RESEARCH ARTICLE

Design, modeling, and preliminary evaluation of a simple wrist-hand stretching orthosis for neurologically impaired patients

Elissa D. Ledoux[1,2], Nithin S. Kumar[1] and Eric J. Barth[1]

[1]Department of Mechanical Engineering, Vanderbilt University, Nashville, TN, USA.
[2]Department of Engineering Technology, Middle Tennessee State University, Murfreesboro, TN, USA.
Corresponding author: Elissa D. Ledoux; Email: elissa.d.ledoux@vanderbilt.edu.

Received: 21 May 2024; **Revised:** 30 September 2024; **Accepted:** 12 October 2024

Keywords: Intelligent orthotics; Rehabilitation robotics

Abstract

This work studies upper-limb impairment resulting from stroke or traumatic brain injury and presents a simple technological solution for a subset of patients: a soft, active stretching aid for at-home use. To better understand the issues associated with existing associated rehabilitation devices, customer discovery conversations were conducted with 153 people in the healthcare ecosystem (60 patients, 30 caregivers, and 63 medical providers). These patients fell into two populations: spastic (stiff, clenched hands) and flaccid (limp hands). Focusing on the first category, a set of design constraints was developed based on the information collected from the customer discovery. With these constraints in mind, a powered wrist-hand stretching orthosis (exoskeleton) was designed and prototyped as a preclinical study (T0 basic science research) to aid in recovery. The orthosis was tested on two patients for proof-of-concept, one survivor of stroke and one of traumatic brain injury. The prototype was able to consistently open both patients' hands. A mathematical model was developed to characterize joint stiffness based on experimental testing. Donning and doffing times for the prototype averaged 76 and 12.5 s, respectively, for each subject unassisted. This compared favorably to times shown in the literature. This device benefits from simple construction and low-cost materials and is envisioned to become a therapy device accessible to patients in the home. This work lays the foundation for phase 1 clinical trials and further device development.

1. Introduction

Neurological events such as stroke and traumatic brain injury affect millions of people across the globe every year (World Stroke Organization, 2022). For many, this results in upper-limb impairment such as lack of hand control, including difficulties grasping and opening, and instability. Customer discovery in the healthcare ecosystem revealed that these are debilitating, life-changing events that leave survivors dependent on others for even the most basic tasks. Over time, their struggles compound, resulting in fatigue, frustration, and a host of additional problems. In addition to physical impairment, interlocutors revealed that they often endure related mental and financial hardships. As a result, patients need a low-cost device to meet their basic needs for gross motor skills recovery and contracture prevention.

Limitations of existing orthoses, as described by therapists and patients in our customer discovery conversations, are rigidity, operation procedure, sizing, and/or cost. Passive orthoses are inexpensive

compared to powered ones but lack the ability to actively move the patient's hand, and either hold it in a static position (static splints) or cause the hand to move unnaturally by coupling wrist motion to finger motion (linkage-based). While elegant in their own right, the powered ones, such as the Myomo, Bioness, GloreHa, and EnableMe (Bioness, 2024; EnableMe, 2015; BTL Robotics, 2024; Kovelman, 2021) are in many cases inaccessible to patients at home due to cost or other factors. The EnableMe and GloreHa are intended for use in a clinical setting with a virtual reality station (EnableMe, 2015; BTL Robotics, 2024). While these can be powerful rehabilitation tools, they are not accessible to patients at home for their daily therapeutic needs. While statistics on cost and weight for most of these powered devices are not publicized, the Myomo is advertised as weighing approximately 2 kg (Kovelman, 2021), more than twice the weight of most research prototypes, and could be difficult for someone with neurological impairment to don and maneuver. The Bioness costs approximately 500 USD (Bioness, 2020), which patients already experiencing financial constraints may find difficult to afford. Neurologically impaired patients need access to low-cost, lightweight, active therapy devices intended for at-home use, in order to enable daily rehabilitation and facilitate their recovery.

Traditionally, exoskeletons and orthoses have been constructed with rigid links and actuation (Ates, 2015; Gasser, 2017; Johnson, 2001; Ueki, 2010). However, over the last decade, research in this area has shifted to the realm of soft robotics due to their human-friendly interaction and novel materials (Tang et al., 2024). Most of the wrist-hand orthoses (WHOs) developed are for assistance (grasping) rather than therapy (stretching), whereas our device is intended for therapy. These WHOs, while developed by different researchers, share many common characteristics of function and form (Saldarriaga et al., 2024). They come in limited sizing, can be difficult for subjects to don (independently or not) due to their glove shape with individual finger slots, and the dynamic ones often pull rather than push the fingers (which can cause tendon issues, according to occupational therapists consulted in this study). Some WHOs are cable-driven by electric motors or linear actuators (Biggar and Yao, 2016; Dragusanu et al., 2024; Li, 2023; Saharan, 2017; Tran, 2022; Yurkewich, 2020), while one (Polygerinos, 2014) is hydraulic, and many others use pneumatic bellows on the dorsal side of the hand (Cappello, 2018; Kladovasilakis, 2022; Lai et al., 2024; Yap, 2017a; Yap, 2017b; Zhao, 2016). The few research prototypes that have been developed for therapeutic stretching purposes (Ates, 2015; Haghshenas–Jarvani, 2020; Shi, 2021; Yap, 2017b) also involve designs complex enough that they require a trained person to assist the patient with donning and use, making it difficult for patients to use them independently at home. Soft orthoses are intrinsically lighter than rigid ones, although all but the lightest ones (Cappello, 2018) still require the hand to support upwards of 120 g. For neurologically impaired patients suffering from weakness and loss of upper-limb motor skills, the lighter an orthosis is, the easier it is for them to use. For patients with stiff, spastic hands, daily stretching is a necessity, and a comfortable and user-friendly therapeutic device could facilitate patients' recovery. Regarding soft, therapeutic WHOs available on the market for at-home use to stretch stiff patient hands, here are two passive orthotic gloves: the SaeboGlove and SaeboFlex (Saebo, 2023a, 2023b). These gloves have springs on the dorsal side of the fingers to passively assist with flexion. While they can be more comfortable than the previously mentioned rigid devices and are available for consumer purchase, they do not provide active (powered) stretching assistance. Due to their design, these gloves can cause excess strain on the tendons and metacarpophalangeal (MCP) joints of the hand by pulling on the fingertips. Furthermore, their sizing is limited, and the individual finger compartments can make it difficult for patients with stiff hands to don and doff. Therefore, patients need the option of an active hand stretching orthosis that is easy to put on and designed to stretch the fingers from the palmar side, in accordance with the preferred method of hand rehabilitation.

Here, the aim is to develop a simple wrist-hand stretching orthosis for stroke survivors and other neurologically impaired patients that is affordable and practical for home use. The authors hope that over time and with frequent use as a therapy tool to meet patients' daily stretching needs in a home setting, this device will eventually help them reduce hand spasticity (stiffness) and regain independence as they regain control of their hands. The prototype subsequently described has been designed using criteria based on the verbalized desires of neurologically impaired patients, their caregivers, and medical providers. This

https://doi.org/10.1017/wtc.2024.22 Published online by Cambridge University Press

device involves a design shift from a typical soft robotic glove structure to a low-profile inflatable vessel. This simple yet novel design effectively employs the principle of pushing rather than pulling the hand open. It is designed to be light and simple enough to be usable by neurologically impaired patients independently and directly addresses their medical needs. This paper presents the design and mathematical modeling of the orthosis, as well as proof-of-concept testing of the prototype on two neurologically impaired patents.

2. Orthosis design

In order to more fully comprehend the upper-limb needs and challenges survivors of neurological events face, and to determine a target end user, the authors conducted informal customer discovery conversations with 153 members of the ecosystem (60 survivors, 30 caregivers, and 63 medical providers) as part of the National Science Foundation I-Corps Program. This customer discovery helped bridge the knowledge gap regarding the generic information and standard of care that is common to the medical community but unbeknownst to many engineers. Discussions with survivors and caregivers yielded additional insights into the unique experiences of individuals from their own perspectives. The authors then realized upper-limb patients fell into two populations: spastic/toned (stiff, clenched hands) and flaccid (limp hands). For the subsequently described body of work, the authors chose to focus on a simple technological solution for the first category of patients. This group struggles to open their hands due to involuntary clenching, or "freezing" of the hands in a curled position, and needs help stretching on a regular basis to relieve their manual tone. Based on the information collected from the customer discovery, the authors developed a set of design constraints and then prototyped a powered wrist-hand stretching orthosis to aid in recovery. The set of design constraints and features derived from customer discovery are as follows:

1. *Easy to don and doff.* Since the patients' hands are stiff, ease of donning is essential. They are unable to control their fingers and must manually push them into position, making individual finger motion practically impossible and often requiring the help of a caregiver in a procedure that can last several minutes. Ideally, a patient could singlehandedly put the orthosis on his hand or remove it in less than 1 min.
2. *Dynamic: flexible and comfortable.* Many patients complained that their static splints are painful due to the constant aggressive stretch, so they need something comfortable or they will not wear it. And since common a side effect of neurological impairment is reduced sensation in the affected limb, preventing abrasion is critical to prevent skin damage and infection.
3. *Therapeutic stretching.* All patients need to stretch their hands to prevent contractures and regain function. To alleviate the mental and physical burdens of constantly opening and closing their hands, and because most patients lack voluntary control, the orthosis should cyclically stretch the affected hand.
4. *Intelligent: intuitive control and sensory feedback.* Any device for a neurologically impaired person must be easy to use and safe. Powering and controlling the device should be simple, and force or pressure monitoring should prevent overextension of joints.
5. *Affordable.* As most neuro patients are no longer able to maintain a full-time job and often require caregiver assistance, they also face financial challenges. A device should be as low cost as possible so they can afford it, ideally below 100 USD.
6. *Portable: lightweight and untethered.* In order for a patient to easily transport and use a device, it must be unchained from external equipment. Furthermore, the proportion of weight on the distal limb should be minimized (ideally <0.5 kg) in order to reduce the required torque to lift the arm and hand, with heavier components located more proximally.

For this prototype, the authors chose to prioritize the first three design constraints: easy to don and doff, flexible and comfortable, and therapeutic stretching. The other design constraints (intelligent,

https://doi.org/10.1017/wtc.2024.22 Published online by Cambridge University Press

Figure 1. *Stretching orthosis prototype. the photos, clockwise from top left, show the prototype with (a) straps unfastened, (b) straps fastened, (c) flat hand, donned, (d) clenched hand, dorsal view, (e) clenched hand, angled view, and (f) clenched hand, palmar view.*

affordable, and portable) will be addressed in future work as the project develops. The orthosis prototype, shown in Figure 1, has a very different form than others in literature. It is essentially an inflatable, intentionally shaped vessel with hook and loop fastener straps. Designing for flexibility and comfort necessitated a soft robotics approach. The vessel is made of nylon coated with TPU, and the stitching and ¼" tubing inlet are sealed with a commercial sealant to prevent leaks. Designed to fit the 50th percentile male hand, but easily scalable to other sizes, the prototype is an hourglass shape 30 cm long, 19 cm wide at the widest part, and 12 cm wide at the narrowest part when deflated. The simple structure facilitates the ease of donning in a way that a standard glove with individual fingers would not. There is one strap for the forearm, two straps for the fingers, and one strap for the thumb. The straps utilize hook and loop fasteners for secure, adjustable positioning and ease of donning and doffing. The finger straps' placement falls on the metacarpophalangeal (MCP) and proximal interphalangeal (PIP) joints of the hand in order to encourage finger extension, as recommended by occupational therapists consulted during the design process. Positioning the finger straps on the joints naturally causes the forces from the straps to intersect the joints, eliminating any torque that would be created by a lever arm, and counteracting (by flattening the fingers) the torque created by the force from the vessel on the fingers. This keeps the knuckles and therefore the links of the fingers in as close contact as possible to the orthosis surface, allowing the fingers to uncurl as the orthosis inflates. The hourglass shape is designed to minimize wasted air while applying sufficient force to open the hand and support the wrist. This wrist support is essential because a patient with spastic hands typically experiences wrist contraction as well, and therefore needs to extend the wrist joint simultaneously with the thumb and fingers. The entire prototype weighs only 63 g, far below the distal weight limit of 500 g and the minimum of other published research prototypes at 120 g (Rahman, 2000). Furthermore, it is quite inexpensive with materials under 5 USD and simply sewn together.

At present, the prototype is actuated via an air compressor, powered through a DC power supply, and controlled through a computer interface, as explained in *section 3.1 Pressure Testing.* This allows for testing device functionality and evaluating the primary design features in a timely manner. A photo of the inflated prototype with dimensions is shown in Figure 2.

https://doi.org/10.1017/wtc.2024.22 Published online by Cambridge University Press

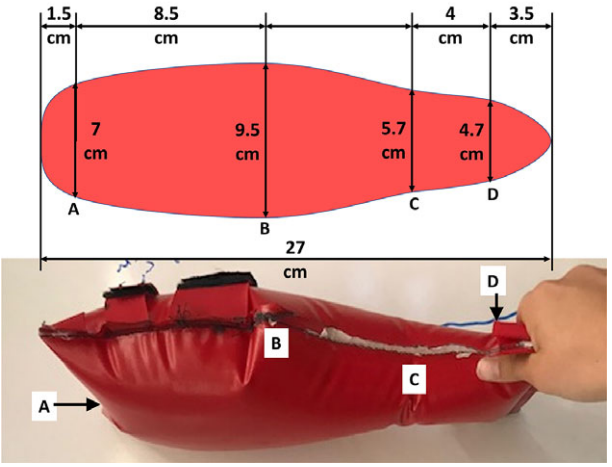

Figure 2. *Inflated orthosis dimensions. The inflated orthosis is on the bottom, and dimensions to certain points are on the top diagram, profile view. The points are: (A) shrink distance of the center due to inflation, (B) the widest point of the hourglass (see Figure 1 a–c), (C) narrowest point of the hourglass (see Figure 1 a–c), and (D) wrist strap. The left end is the distal end, and the right is proximal.*

3. Experimental testing and results

Two neuro-patient test subjects were recruited from a brain injury rehabilitation clinic through the recommendation of an occupational therapist. One subject was an elderly male just over a year post-stroke, who displayed medium hand spasticity (tone). The other subject survived a traumatic brain injury (TBI) nearly 2 years prior and had a lower tone as perceived by the authors. Details about each subject are shown in Table 1. The baseline Modified Ashworth Scores (MAS) for each subject was assessed separately for the digits (fingers and thumb) and wrist by the clinic and are reported on a 0 (best) to 4 (worst) scale. The study was approved by the Vanderbilt University Institutional Review Board, study number 221203, and all subjects provided informed consent to participate.

Each subject came separately to the lab to test the orthosis. Three types of tests were performed: donning and doffing, grip force, and cyclic stretching. The full sequence of events for each session is enumerated below, and the tests are specified in a graphic in Figure 3. Video footage of the testing is available here.

1. Allow the subject to acclimate to the orthosis;
2. Measure initial resting and maximum grip forces;
3. Don orthosis (time);
4. Measure inflation pressure required to open hand;
5. Cyclically inflate/deflate orthosis to stretch hand;
6. Doff orthosis (time);

Table 1. *Test subject information*

	Subject 1	Subject 2
Injury	Stroke	TBI
Months post-injury	14	20
Gender	Male	Male
Age (years)	74	37
Tone level	Medium	low
Digits MAS	3	3
Wrist MAS	2	3

https://doi.org/10.1017/wtc.2024.22 Published online by Cambridge University Press

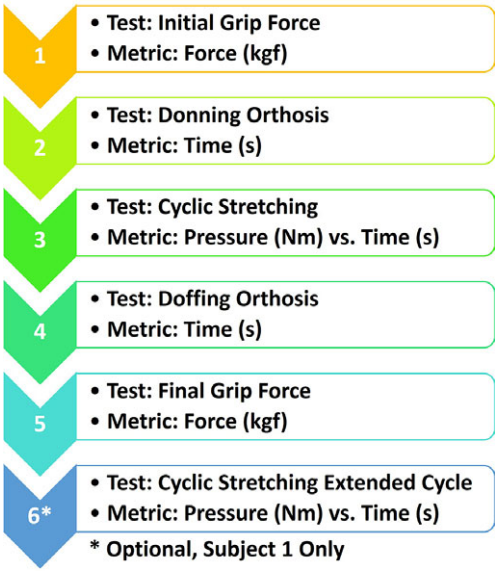

Figure 3. *Testing sequence. This graphic outlines the experimental protocol for subject testing.*

7. Interview subject for feedback;
8. Measure final resting and maximum grip forces;
9. Optional: Cyclically inflate/deflate orthosis to stretch the hand on a longer cycle.

3.1. Donning and doffing

The donning and doffing tests consisted simply of the subject strapping the orthosis on their arm and then removing it. After an acclimation period, during which a subject could "practice" with the orthosis until he verbalized readiness for testing, each subject was timed for the procedures and observed to determine if he could complete them independently. Both subjects were able to don and doff the orthosis without assistance. Their donning and doffing times are listed in Table 2.

3.2. Pressure testing

The authors constructed a setup to regulate and measure air pressure in the orthosis during the experiments. A diagram of this setup is shown in Figure 4. An air line was connected to a Festo proportional directional control valve (MPYE-5-M5–010-B), powered by a 24 V DC supply and controlled by Simulink Real-Time via a Humusoft data acquisition card (MF634). The valve was connected to an analog pressure sensor (Festo SDE-16-10 V/20 mA), which was attached to the orthosis via ¼" pneumatic tubing. First, a pressure regulator on the pressure supply line was opened, and then the pressure was slowly and manually increased to inflate the prototype until the subject's hand opened (see Figure 5). The regulator was then set as the desired peak pressure for the open loop cyclic stretching tests.

Table 2. *Donning and doffing times*

Subject	Don time (s)	Doff time (s)
Subject 1	82	12
Subject 2	70	13

https://doi.org/10.1017/wtc.2024.22 Published online by Cambridge University Press

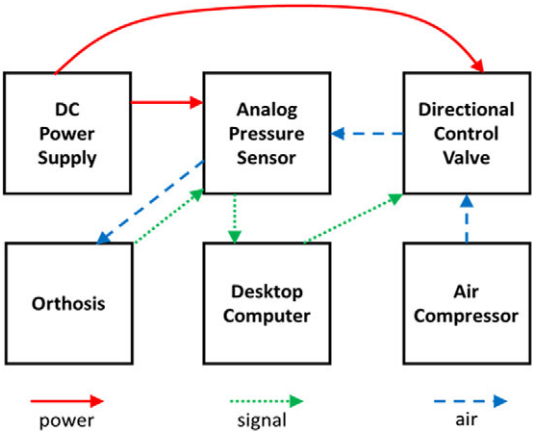

Figure 4. *Experimental setup. This block diagram shows the experimental setup. The arrows indicate the flow of power (red, solid), signal (green, dotted), and air (blue, dashed) for device inflation.*

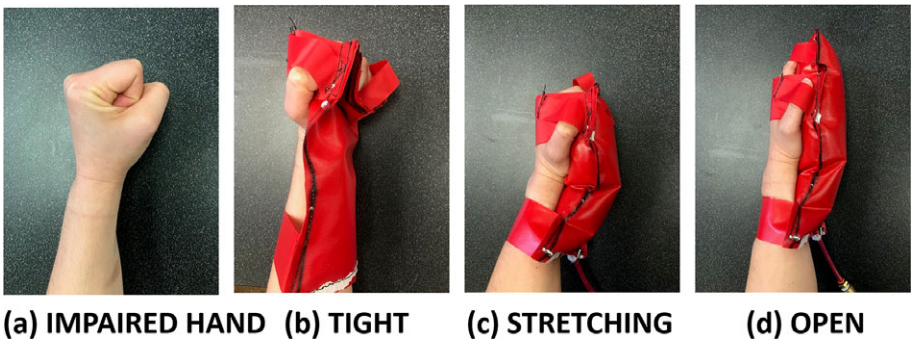

Figure 5. *Hand stretching cycle. The first photo shows a spastic hand, and the remaining three show how the hand opens as the orthosis inflates.*

The primary cyclic stretching test involved five, 1-min sessions in which the prototype was inflated and deflated over a 4-s cycle of sinusoidal valve orifice position. The subjects alternated between 1 min of stretching and 1 min of resting for a total of five sets. During the test, each subject was carefully observed and communicated with to ensure his hand was not in pain. At the suggestion of the occupational therapist, an additional (optional) test was appended to the protocol, using a longer cycle (3 min of a 12-s cycle biased toward inflated: 8 s inflate, 4 s deflate). With Subject 1, five sets of this were intended to be completed, but during the fourth set, he complained of hand soreness where the stitching on the straps contacted his skin, so the test was discontinued, and Subject 2 was not asked to participate in this supplemental test during his visit.

Pressures required for the orthosis prototype to open each subject's hands are shown in Table 3. A higher tone corresponded to higher opening pressure.

For each subject, during the main cyclic stretching test, the orthosis took approximately three cycles to fully inflate, at which point it continued cycling at a steady state. Performance averages over 10 steady-state stretching cycles are shown for each subject for the first and last (fifth) 1-min session in Figure 6. One can see that the performance consistency increased between the first and last tests as each subject's hand relaxed, suggesting that the orthosis can facilitate consistent, repeatable motion.

https://doi.org/10.1017/wtc.2024.22 Published online by Cambridge University Press

Table 3. *Opening pressures*

Subject	Tone level	Opening pressure
Subject 1	Medium	5 psig
Subject 2	Low	4 psig
Empty device	n/a	3.5 psig

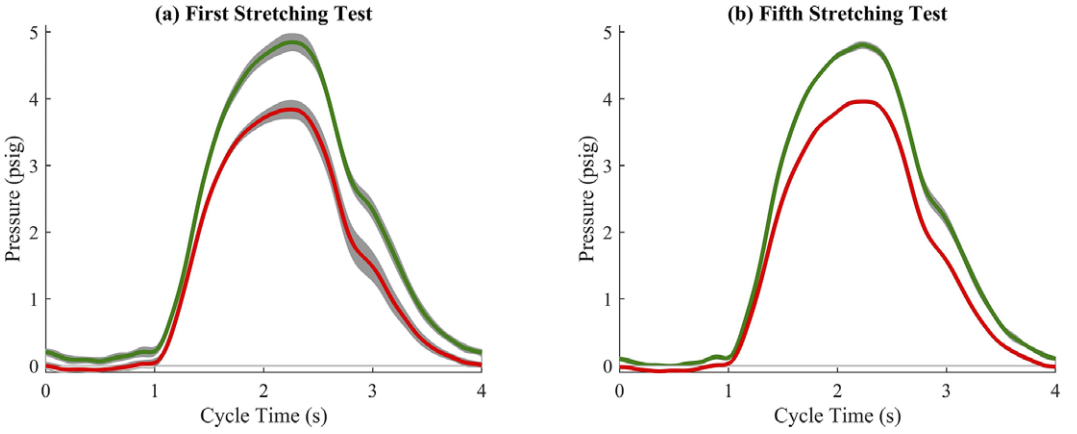

Figure 6. *Stretching pressures. These figures show the average air pressure in the orthosis over 10 cycles for (a) the first one-minute interval, and (b) the last (fifth) one-minute interval. Subject 1's curve is green, and Subject 2's curve is red. The gray bands indicate ± 1 standard deviation from the means. The standard deviation bands are too small to be seen on the fifth session (b) for both subjects, indicating that consistency increased between the first and last intervals.*

3.3. Grip force

Grip force testing was conducted at the beginning and end of each session to see if stretching the hand affected grip force. Force was measured with a digital hand dynamometer and reported in kilograms. Two types of forces were measured: "resting" grip force to determine the tension in the affected hand, and maximum grip force to quantify how much force the subject could voluntarily exert with the same hand. Resting and maximum grip forces before and after stretching are shown in Table 4 for each injured subject and each session. Subject 1 was tested twice because no significant grip force reduction was observed after the original session. The hand dynamometer does not register forces less than 1 kg, so any force below that threshold is indicated as "< 1".

In order to estimate the maximum possible forces the orthosis could endure, a strong, healthy subject was also tested. This subject was a 25-year-old male rock climber selected for his superior grip strength. First, his maximum grip strength was measured with the hand dynamometer. After resting, he was then instructed to don the orthosis and clench it in his fist as tightly as possible, while the inflation pressure was slowly increased until either the prototype ruptured or the hand opened. When testing maximum pressure with a strong healthy subject, the prototype withstood the subject's grip. It inflated to 35 psi without rupturing, at which point the subject complained of pressure from the edge of the strap against his hand,

Table 4. *Grip force before and after stretching*

Subject, session	Resting, before (kgf)	Max, before (kgf)	Resting, after (kgf)	Max, after (kgf)
Subject 1	1.2	8.1	< 1	7.9
Subject 2	< 1	8.8	< 1	5.7
Healthy subject	N/A	55	N/A	N/A

https://doi.org/10.1017/wtc.2024.22 Published online by Cambridge University Press

and the test was discontinued. The maximum grip force of this strong healthy subject was 55 kgf and is included in Table 4.

3.4. Subject feedback

Following the testing, the subjects were informally interviewed to determine their perspective on the orthosis and testing session. The authors wished to determine what the subjects liked about the device, how it could be improved, and if they had any additional suggestions for device or protocol development. Both test subjects remarked on the comfort of the orthosis prototype, due to its flexible structure yet stable straps. Additionally, they both expressed approval for the strap design contributing to ease of donning. Neither subject complained of discomfort during or after the 5-minute stretching test as long as the orthosis was properly positioned on the hand. During Subject 1's additional (extended) stretching test, he expressed feeling soreness at 11 min, at which point the test was terminated and the orthosis removed. Upon inspecting his hand, the skin on the dorsal side was tender to the touch and sustained marks from the stitching on the straps. The residual discomfort did not last long or dampen his enthusiasm for the device, and it was concluded that stretching sessions should be kept to 10 min or less in order to avoid possible discomfort and that the stitching on the device should be lower profile to avoid abrasion.

4. Mathematical modeling

A lumped parameter model was developed to describe the compliance of the hand (quantify the stiffness of the fingers) based on the experimental kinematic data and orthosis pressure. This model will be useful for determining joint stiffness as a metric to quantify and monitor patient improvement over time. Ideally, joint stiffness would decrease as the patient consistently performs therapeutic stretching and exercises for recovery. This model is two-dimensional (in the sagittal plane) and discretizes the hand as rigid links that are sequentially connected and able to rotate in the plane in the presence of applied and internal forces and moments. This simplification is justified because the finger diameter is sufficiently smaller than the hand length and depth. This model is derived by lumping all four fingers as one and only considering the three segments of this lumped finger along with the palm. In particular, we treat each link as having a center of mass and a rotational moment of inertia corresponding to a slender rod. Each link is tied to its neighboring links with rotational springs and damping terms to represent angular compliance and resistance. As the orthosis inflates, each link is subject to a normal force. This is modeled as an equivalent external force and is computed by the product of the equivalent pressure-induced force and resultant area (product of link length and depth of lumped finger/wrist system), applied at the center of each link. The coordinate system and free-body diagram of the system are shown in Figure 7.

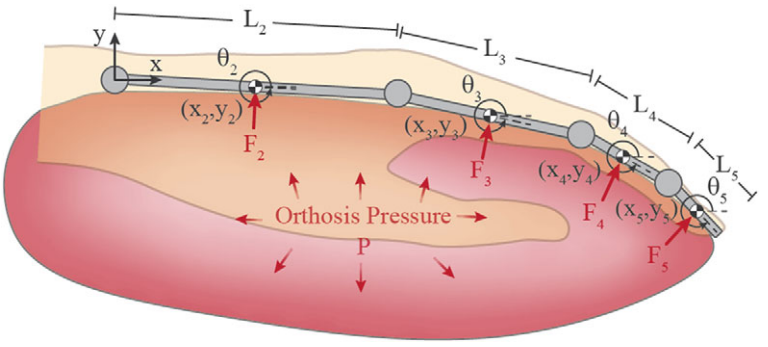

Figure 7. *WHO modeling diagram. this diagram shows the 4-link model of the hand, along with states used to represent this system. The inflated orthosis is depicted in red along with the resultant pressure forces acting at the center of each link. The forearm link (L_1) is grounded and not shown in this diagram.*

https://doi.org/10.1017/wtc.2024.22 Published online by Cambridge University Press

In this work, we use a maximal generalized coordinate representation to describe the system. The states q for this model for links i = 2–5 include:

$$q = [x_2, y_2, \theta_2, \ldots, x_5, y_5, \theta_5]^T \tag{1}$$

where x_i and y_i are the position of the respective link center, and θ_i is the link angle with respect to a global frame as shown in Figure 7. The dynamics of the system are derived using a constrained Lagrangian approach. Consider a set of constraints of the form $\phi(q) = 0$ representing the constraints that tie the links together at the joints. The associated Lagrangian L is given by $L = T - V + \phi^T \lambda$, where T is the total kinetic energy of the system, V is the total potential energy, ϕ is the set of constraint equations, and λ is the vector of Lagrange multipliers. The dynamics of the system are formulated as:

$$\frac{d}{dt}\left(\frac{\partial L}{\partial \dot{q}_i}\right) - \frac{\partial L}{\partial q_i} + \sum_{j=1}^{8} \lambda_j \frac{\partial \phi_j}{\partial q_i} = 0 \tag{2}$$

There are a total of 8 constraints in this system. There are six constraints that ensure link-to-link continuity by relating the positions of consecutive centers of masses. These equations describe the hinge point ahead of the center of mass of the i^{th} link, and behind the $(i+1)^{th}$ link as the same points and are given as:

$$x_i + \frac{L_i \cos(\theta_i)}{2} + \frac{L_{i+1} \cos(\theta_{i+1})}{2} - x_{i+1} = 0 \tag{3}$$

$$y_i + \frac{L_i \sin(\theta_i)}{2} + \frac{L_{i+1} \sin(\theta_{i+1})}{2} - y_{i+1} = 0 \tag{4}$$

To pin one end of L_2 to the origin of the coordinate system, x_2 and y_2 are each constrained such that:

$$x_2 - \frac{L_2 \cos(\theta_2)}{2} = 0 \tag{5}$$

$$y_2 - \frac{L_2 \sin(\theta_2)}{2} = 0 \tag{6}$$

The system of equations can be formulated in matrix form as follows:

$$M\ddot{q} + A^T \lambda = F \tag{7}$$

Here M is the diagonal inertia matrix containing link masses and moments of inertia, A is the sparse constraint matrix given by $A = \frac{\partial \phi}{\partial q}$ of size 8×12, and F collects all internal and external generalized forces and torques. For a detailed derivation of this model, refer to (Rucker, 2022). Baumgarte stabilization (Baumgarte, 1972) was implemented to ensure constraints were numerically enforced over simulation runtime. Without such an enforcement scheme, constraint equations may be violated due to the accumulation of integration truncation errors (Flores, 2011; Haizman, 2007). The stabilized constraints were derived by differentiating the set of original constraint equations twice:

https://doi.org/10.1017/wtc.2024.22 Published online by Cambridge University Press

$$\phi(q) = 0,$$
$$\dot{\phi}(q) = \frac{\partial \phi}{\partial q} = A(q)\dot{q} = 0,$$
$$\ddot{\phi}(q) = A(q)\ddot{q} + \dot{A}(q)\dot{q} = 0,$$

and incorporating them into a stable 2nd order dynamic relationship that rapidly brings any constraint violations to zero by choosing appropriately fast and damped parameters ζ and ω_N:

$$\ddot{\phi}(q) + 2\zeta\omega_N\dot{\phi}(q) + \omega_N^2\phi(q) = 0$$

$$A(q)\ddot{q} = -\dot{A}(q)\dot{q} + 2\zeta\omega_N\dot{\phi}(q) + \omega_N^2\phi(q) = 0 \tag{8}$$

The combined set of equations (7) and (8) describe the evolution of the states (1) and are solved simultaneously:

$$\begin{bmatrix} M & A^T \\ A & 0 \end{bmatrix} \begin{bmatrix} \ddot{q} \\ \lambda \end{bmatrix} = \begin{bmatrix} F \\ \gamma \end{bmatrix}. \tag{9}$$

Here, $\gamma = -A(\dot{q})\ddot{q} - 2\zeta\omega_N A(q)\dot{q} - \omega_N^2\phi(q)$ and F is the sum of internal (F_{int}) and external (F_{ext}) generalized forces. In particular, the generalized internal torques in F are of the form:

$$F_{\theta_{i,int}} = K_i(\theta_i - \theta_{i-1} - \theta_{i,i-1,0}) + K_{i+1}(\theta_{i+1} - \theta_i - \theta_{i+1,i,0}) - B\dot{\theta}_i$$

Here K_i is the rotational spring constant of the i^{th} joint and B is a damping coefficient implemented for faster convergence. The $K_i(\theta_i - \theta_{i-1} - \theta_{i,i-1,0})$ term reflects the rotational spring torque generated from the deviation of the proximal joint from its equilibrium position, given by the constant $\theta_{i,i-1,0}$. Similarly, $K_{i+1}(\theta_{i+1} - \theta_i - \theta_{i+1,i,0})$ represents the rotational spring torque from the distal joint. The generalized external forces (due to the orthosis) in F are given by:

$$F_{x_{i,ext}} = -F_{orth,i}\sin(\theta_i)$$

$$F_{y_{i,ext}} = -F_{orth,i}\cos(\theta_i)$$

The external force for link i, $F_{orth,i}$, is a product of the pressure in the orthosis and the effective area that contacts the orthosis at each link. These forces are applied normally to each link, and their effective contact areas are given in Table 5.

The goal of this modeling work is to determine the rotational spring constants K_i of each joint. This was done by numerically integrating the system of equations (9) in MATLAB 2022b using the ode15s solver

Table 5. *Effective contact area*

Joint	Effective area $A_e(mm^2)$
Wrist	4750
MCP	3500
PIP	1960
DIP	1680

https://doi.org/10.1017/wtc.2024.22 Published online by Cambridge University Press

with an initial random set of K_i (all set to 1 Nm/rad). The configuration error, e, defined as the difference between the desired and steady-state joint angle values (after all dynamics settle), was used to find a new set of K_i iteratively until the sum of squared errors fell below a certain threshold (set at 0.05) as follows:

$$K_{i,new} = K_{i,old} - Ce \tag{10}$$

where C is a positive constant, proportional to the magnitude of $(K_{i,old})$ to help with convergence. The intuition for the negative sign is that if the error is positive, the current joint needs to be less stiff to reach the desired angle. It should be pointed out that this has no physical interpretation, per se; it is merely a numerical method for finding the joint stiffnesses that match the simulation's configuration to the physically observed configuration. The initially curled hand position is set as the spring equilibrium position for each link. As the orthosis inflates, the links straighten to a final position. The orthosis is modeled as a constant-perimeter balloon constrained maximally to the inflation dimensions (see Figure 2).

To first validate this modeling approach, and verify that it yields reasonable stiffness values, a mechanical hand was designed, 3D-printed, and integrated with springs with known stiffness values (see Figure 8).

It was empirically observed that the inflated orthosis does not provide additional force on the hand beyond a certain angle, due to the fact that the surface is convex when inflated. In particular, this effect is more significant on the distal joints. A healthy subject's joint angles resting on the orthosis were used to estimate an "offset" angle for each link (i.e., the orthosis does not provide a force on any link that is larger than a certain, empirically derived angle). This effect was modeled as a linear decrease in the pressure exerted by the orthosis from the initial configuration of each link to the estimated offset angle. For example, an offset angle of $\alpha > 0$ modifies $F_{orth,i}$ to:

$$F_{orth,i} = P\frac{(\theta_i + \alpha)}{(\theta_{i,0} + \alpha)}A_{e,i} \tag{11}$$

Here P is the gauge pressure in the orthosis, $\theta_{i,0}$ is the initial angle of the joint and $A_{e,i}$ is the effective area of the corresponding joint. The term $\left(\frac{\theta_i+\alpha}{\theta_{i,0}+\alpha}\right) = 1$ at the initial joint configuration $\theta_i = \theta_{i,0}$ and

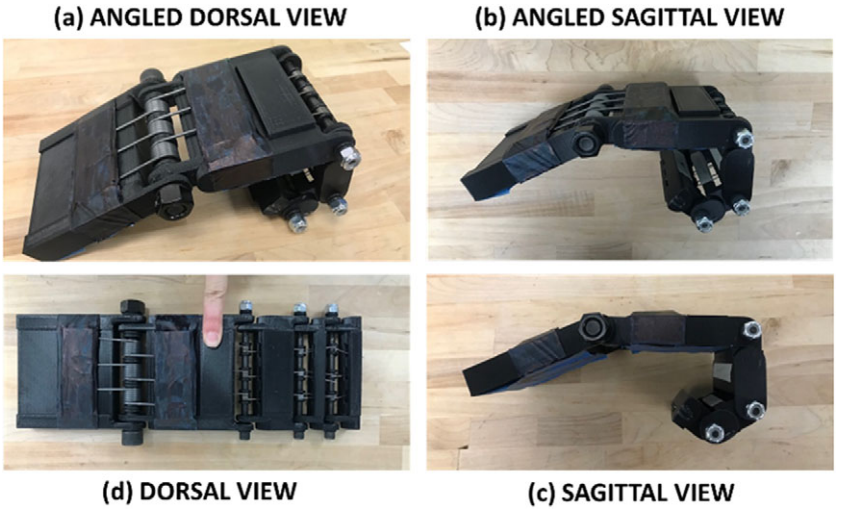

Figure 8. *Mechanical hand. This figure shows the phantom hand prototype, constructed of 3D-printed ABS links, connected by revolute joints with torsional springs of known stiffnesses.*

https://doi.org/10.1017/wtc.2024.22 Published online by Cambridge University Press

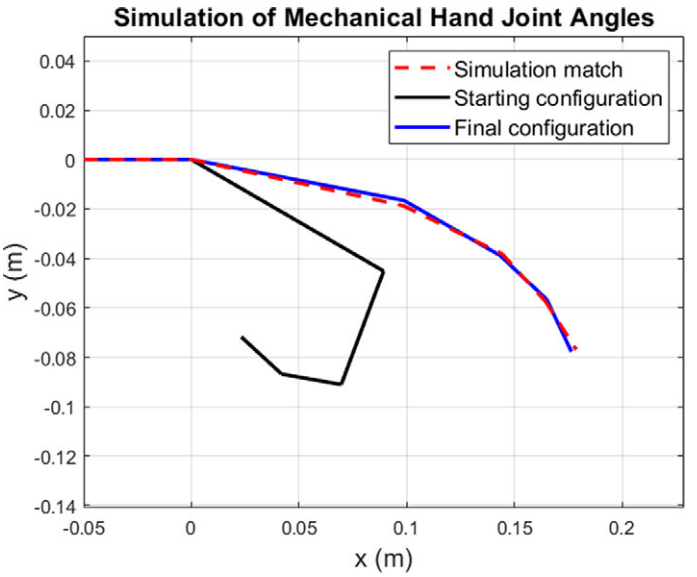

Figure 9. *Simulation results of final configuration static matching of the 3D printed mechanical hand. Known spring constants are used to show the predicted and actual mechanical hand configuration. The average rotation error is 4.1 deg (magnitude of 1.2, 3.5, 4.3, and 7.6 deg for each joint, from the wrist to the DIP, respectively).*

represents the maximum force applied to the joint. When $\theta_i = -\alpha$, the expression reduces to 0 and describes the scenario when the orthosis is unable to exert any additional force on the joint. Note $\theta_i < 0$ for all angles as shown in Figures 9 and 11. Offset angle values of 10, 30, 30, and 45 degrees were used for the wrist, MCP, PIP, and DIP joints respectively, and we find there is reasonable agreement between the simulation and the experimental configuration of the mechanical hand, as shown in Figure 9. The average rotation error is 4.1 deg (magnitude of 1.2, 3.5, 4.3, and 7.6 deg for each joint, from the wrist to the DIP, respectively).

After validating the modeling approach on the mechanical hand, the analysis was then extended to determine joint stiffnesses of a test subject's impaired hand. Using photographs from Subject 1's testing, the link lengths and initial and final relative link angles were determined (see Figure 10 for an example). The mass of the hand was estimated to be 0.5 kg (corresponding to the 50th percentile male hand mass), with the weight distributed between the palm and fingers at a 60:40 ratio and the finger segments' mass proportional to length. These values were used in combination with the measured inflation pressure of the orthosis (5 psig) to simulate the hand opening and determine joint stiffnesses.

Figure 11 plots the experimental starting configuration in black, the experimental (desired) final configuration in blue, and the simulation match based on the iteratively-derived spring constants in red. Here the average rotation error is 0.7 deg (0.2, 1.5, 0.39, and 0.59 deg for each joint, from the wrist to the DIP, respectively).

Simulation results indicate joint stiffness decreasing from proximal to distal for this patient-specific data. The relative angle changes for each joint, as well as the stiffness values, are shown in Table 6. Angle changes are all negative due to the hand straightening.

5. Discussion

The flexibility and motion of the device improve upon the static splints currently in use, and the wrist support and ease of donning improve upon other research prototypes. Specifically, because the device is essentially a thin bag, it can be crumpled into a clenched fist, which makes it easier for patients to don and

https://doi.org/10.1017/wtc.2024.22 Published online by Cambridge University Press

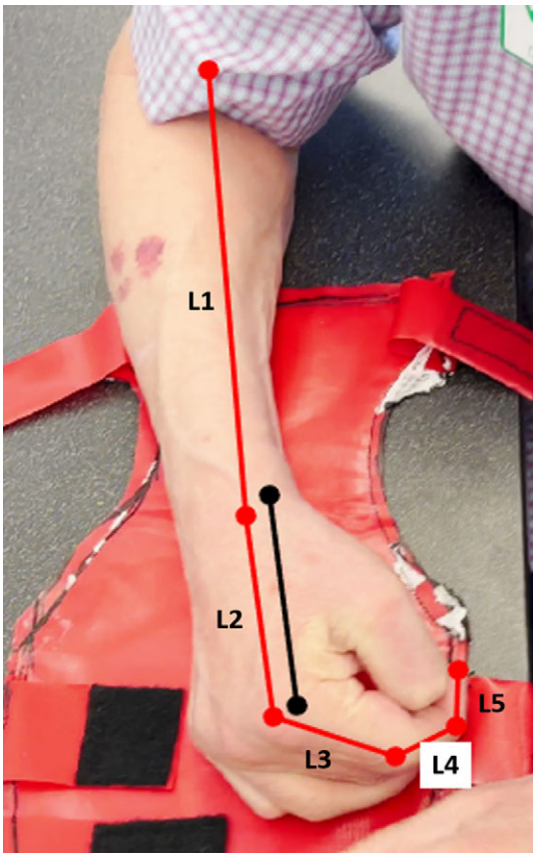

Figure 10. *Subject dimensions. This figure shows the segment data for a subject's hand prior to stretching. The black line is a known distance of 100 mm used for calibration, and the red lines indicate link lengths (forearm L_1, dorsal palm L_2, proximal finger segment L_3, middle segment L_4, and final segment L_5).*

doff than others in the literature. Additionally, the approach of extending the hand by applying outward pressure from within the clenched fist is preferred by therapists compared to conventional devices that pull the fingers open from the outside (EnableMe, 2015; BTL Robotics, 2024; Saebo, 2023a, 2023b). Furthermore, both test subjects and the occupational therapist expressed approval for the device design and performance.

The goals for donning and doffing were for the subjects to do each independently in under a minute. These goals were neared or exceeded. Both subjects were able to put on and remove the orthosis without assistance. In addition to the flat design of the device that was able to be donned by placing the hand on top of the device, they expressed approval of the strap design for ease of donning. Their times for donning were between 1 and 1.5 mins each, which are acceptably close to the 1-min goal and have the potential to improve with practice (that is if this were a take-home device). Removing the orthosis was much faster than donning, and both subjects did so easily in under 15 s. These results in particular stand out relative to existing research prototypes, which are more difficult to don and doff due to individual finger attachments. The minimum currently published times for donning and doffing are 3 min and 23 s, respectively, (Yurkewich, 2020) approximately twice that of the prototype described here. Existing literature states only the times for donning and doffing and not the level of assistance patients received.

As shown in Table 2, the required pressure to open the subjects' hands increased with increasing tone. These results make sense and are further corroborated by the fact that the orthosis took the least amount of

https://doi.org/10.1017/wtc.2024.22 Published online by Cambridge University Press

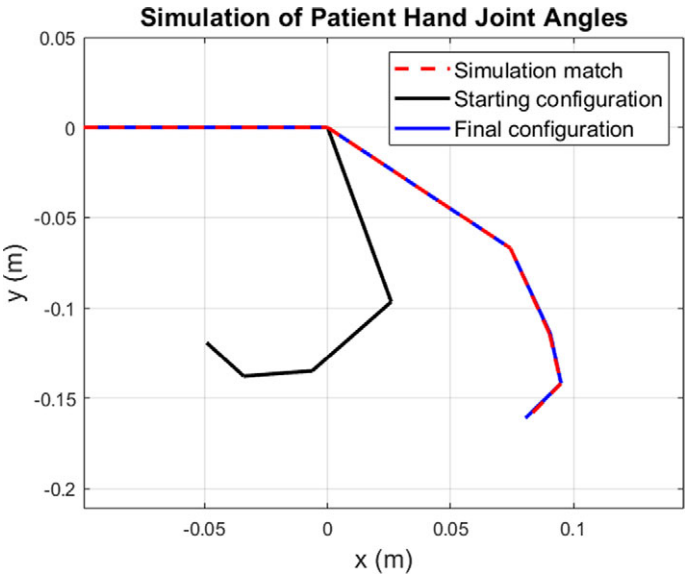

Figure 11. *Simulation results of final configuration static matching for a patient's hand. The controller can drive the simulation (red dashed line) from the starting configuration (black) of the closed hand to the final (blue) configuration by identifying sufficiently accurate joint stiffness values. Here the average rotation error is 0.7 deg (0.2, 1.5, 0.39, and 0.59 deg for each joint, from the wrist to the DIP, respectively).*

Table 6. *Joint angles and stiffnesses*

Joint	$\theta - \theta_0$	k (Nm/rad)
Wrist	−4	32.4
MCP	−22	12.3
PIP	−40	2.4
DIP	−9	1.7

pressure to inflate without a hand in it. Based on the maximum pressure test results and its performance throughout the testing session, the orthosis prototype can exceed the strength required to open a toned hand by an order of magnitude, while also offering the safety of being incapable of overextending finger joints. The pressure required to open the injured subjects' affected hands ranged from 4–5 psig, and the prototype was able to inflate to 35 psig without rupturing. Although the manual tone of the subjects tested ranged from low to medium, the range of allowable pressures is such that the prototype should be sufficiently strong enough to stretch hands with a more aggressive tone as well.

During cyclic stretching, the orthosis behaved consistently, as evidenced by the small standard deviations in pressure. Furthermore, it is clear that the performance became even more consistent from the first to the last tests as the subject's hand relaxed. In fact, on the last tests, the standard deviation is so small that the difference between cycles (evidenced by the gray band) is barely visible. The pressure curves are also as expected for a nonlinear, constant surface area system. One can see that pressure is essentially zero until the orthosis is full of air, and then observe a swift increase in pressure as the volume remains fairly constant. The actual pressure peaks close to the desired magnitude with a slight (approximately 0.5 s) lag, and then decreases with input pressure. It is important to note that no vacuum was applied, only an exhaust valve was slowly opened, so any air leaving the orthosis was due to the subject's hand naturally contracting to push it out. Per visual observation, the hand became significantly straight with the orthosis fully inflated, and it contracted back near its original level as the pressure was

https://doi.org/10.1017/wtc.2024.22 Published online by Cambridge University Press

removed. The vessel did not completely empty during deflation, which is beneficial because that means the subject's hand did not completely close (an undesirable position). Exact joint angles were difficult to quantify during the cycle, simply due to the vessel and straps obscuring parts of the hand.

The grip force test results were inconclusive as to the effects of manual stretching on grip force. Maximum grip force decreased substantially for Subject 2 after stretching, but not for Subject 1. The reasons for this are unknown, but it could be because Subject 2 had a lower tone, and so his hand was easier to relax. It is also noteworthy that Subject 1 was overly competitive with trying to exceed his previous measurements and peek at the numbers, while Subject 2 did not attempt to do so. Overall, changes in grip force are inconclusive. It remains unknown if the orthosis can offer a short-term therapeutic benefit, as grip force may have a longer-term effect. More testing is needed to investigate whether short-term therapeutic benefits are possible and/or if longer-term use will offer benefits.

Both subjects had positive feedback regarding the orthosis and testing experience. They said the device is something they would use both at home and in public with no qualms, due to an eagerness to facilitate their recovery. Subject 1 was particularly enthusiastic, asserting that it was a "fabulous stretching concept that could really open up possibilities," and he would take "any chance for improvement, I need to practice every day for results." Both subjects speculated on the potential benefits of the orthosis for facilitating activities of daily living, as less stiff hands could enable them to regain independence and efficiency with many activities. They specifically mentioned cooking, cleaning, eating, and opening water bottles as desired abilities that this device could hasten.

The occupational therapist consulted throughout the prototype development and study process had positive feedback and helpful insights. She praised the concept and effectiveness of the orthosis prototype for gently stretching stiff hands via pushing with a distributed load rather than pulling on the fingertips (Rehab and Tran, 2022) (an often overlooked issue which could cause irreparable musculoskeletal damage). She also spoke approvingly of the strap placement in locations conducive to muscle relaxation, and the fact that the orthosis supports the wrist in addition to the hand because an affected wrist tends to contract/curl as well. Regarding use, the therapist said she would recommend this device for at-home use with manually impaired patients two to three times per day for light stretching (up to 15 min) before performing a manual activity. She also recommended that future control involve a longer stretching cycle biased toward "open", for example, 8 s inflated and 4 s deflated for a 12 s cycle. The therapist also informed the authors that hand spasticity can be affected by a gamut of factors, including temperature, pressure, how much sleep someone had, mental state, etc., and so can vary from day to day (Burke et al., 2019; Sunnerhagen et al., 2019). She acknowledged that stretching and using the hand helps substantially but is not the only factor in recovery or performance, and patients must practice daily for best results.

The effect of mental state on hand spasticity was directly observed with Subject 1 early in the session. When asked to don the device for the first time, the subject struggled for a while with a very stiff hand and told the authors he was nervous in front of them. The authors then distracted him via conversation, and saw that his affected hand visibly relaxed. After the subject had acclimated to the orthosis and the lab environment, the official tests began and were easily completed.

A constrained Lagrangian formulation was used to model a hand as a set of sequential rigid links with torsional compliance and damping. Simulation results indicate that stiffness decreases toward the distal joints for a single patient test case. Model validation with a 3D printed mechanical hand and known stiffness constants indicate that this model is a potentially useful tool to quantify and monitor changes in patient joint stiffness. One limitation of this modeling approach is that though the wrist is one joint, each lumped finger joint is based on four separate fingers with non-collinear axes and lengths. A higher fidelity model could be used to determine the spring constants of each finger joint by extending this work to three dimensions and modeling each finger separately, but this approach was determined not to provide significant additional benefit since the current device cannot separately exercise each finger, and so was not pursued. A second limitation of this approach is that all the measurements obtained are approximate due to the joint collinearity approximation. Additionally, this was only done on one patient, so the precise joint stiffnesses do not extend beyond the subject. However, it is not the exact joint stiffnesses that are of importance, but rather the relative joint stiffnesses and changes over time. The

https://doi.org/10.1017/wtc.2024.22 Published online by Cambridge University Press

benefit of the modeling is in the ability to characterize each patient's hand stiffness at each therapy session, thereby monitoring progress. Ideally, patient hand stiffness would decrease over time as they recover, so therapists could use this approach to ascertain and quantify progress beyond the typical qualitative assessment.

The primary limitations of this study are the low number of test subjects and brief time span. Although two test subjects are considered sufficient for validating a proof-of-concept design for engineering, the results obviously do not have statistical power and therefore do not generalize to the entire neurologically impaired population. Also, a 5 to 10 minute stretching session is not long enough to measure chronic benefits of the orthosis. Future work on the engineering side would be to advance the prototype to the point that it could be used in a clinical or even a home setting, where participants would have daily access. Then clinical researchers could measure its effects on a greater number of participants over several months to determine more generalized and long-term benefits.

6. Conclusion

The design of the stretching orthosis prototype is simple and effective, solving some issues with existing technology and current research. The primary design considerations of easy to don, soft, inexpensive, and therapeutic stretching have been met. Because of the prototype's soft and thin material, its low weight of only 60 g, and the absence of individual finger compartments, neurologically impaired patients with stiff hands were able to don it fully unassisted and twice as quickly as any in current literature. Patients also appreciated the comfort of the soft material and cyclic pressure compared to their conventional rigid, static splints. During the hand stretching experiment, as the prototype caused the patients' hands to relax, the cyclic pressure profile became more consistent over time, to the point that variance was barely discernible, underscoring its consistent, comfortable and smooth operation. A dynamic model was developed to characterize the lumped joint stiffness of both a 3D printed and a patient's hand. The model was formulated by assuming a hand as a set of elastically linked rods and calculating the stiffness of each joint due to the force exerted by the orthosis, given known initial and final joint angles. This framework has the potential to be used as a diagnostic metric to quantitatively evaluate patient joint flexibility over time. The initial evaluation of functionality in this T0 preclinical study sets the stage for further prototype development and evaluation of long-term effectiveness in a Phase 1 clinical trial. Future prototype development will involve addressing the remaining design constraints of portability with on-board power and control, and a target total mass of 1 kg, located primarily proximal to the body on the upper arm.

Acknowledgments. The authors would like to thank the test subjects for their participation in the study, as well as Valery Hanks, occupational therapist at Pi Beta Phi neurological rehabilitation center, for her advice on device design and testing. We would also like to thank Kim Sung for his help with Figure 6.

Data availability statement. Derived data supporting the findings of this study are available from the corresponding author upon reasonable request. Certain data such as subject names and contact information will not be available due to privacy requirements.

Author contribution. E.D.L. and E.J.B. conceived of and designed the work. E.D.L. and E.J.B. conducted customer discovery to inform the prototypes. E.D.L. designed the hardware prototypes, recruited the test subjects, and collected the human subject data. N.S.K., E.D.L.,and E.J.B. processed, analyzed, and modeled the human subject and mechanical hand data. E.D.L., N.S.K., and E.J.B. analyzed and interpreted the data. E.D.L. wrote most of the original draft, N.S.K. wrote the modeling section, and all authors revised and approved the final manuscript.

Funding statement. This research was supported in part by grants from the National Science Foundation (TI-2120154 and EFMA-1935278).

Competing interest. None.

Ethical standard. The research meets all ethical guidelines, including adherence to the legal requirements of the United States for human subjects research. This study was approved and registered under the Vanderbilt University Institutional Review Board study number 221203. This manuscript is revised from the preprint version on TechRxiv, (Ledoux et al., 2023) and it is not under review for any other journal.

https://doi.org/10.1017/wtc.2024.22 Published online by Cambridge University Press

References

Ates S, et al. (2015) Combined active wrist and hand orthosis for home use: lessons learned. In *IEEE ICORR*. https://doi.org/10.1109/ICORR.2015.7281232

Baumgarte J (1972) Stabilization of constraints and integrals of motion in dynamical systems. *Computer Methods in Applied Mechanics and Engineering*, **1**(1), 1–16.

Biggar S,&**Yao W** (2016) Design and evaluation of a soft andwearable robotic glove for hand rehabilitation. *IEEE Transactions on Neural Systems and Rehabilitation Engineering*, **24** (10), 1071–1080. https://doi.org/10.1109/TNSRE.2016.2521544

Bioness (2024) H200 for hand paralysis, Product Information, Encompass Health Corporation.

BTL Robotics (2024). R-Lead: Neurocognitive Training for Upper Limbs, BTL Corporate, https://www.btlnet.com/r-lead.

Burke D, **Wissel Jand Donnan G** (2019) Pathophysiology of spasticity in stroke. *Neurology* **80**. S20–26. https://doi.org/10.1212/wnl.0b013e31827624a7

Cappello F, et al. (2018) Assisting hand function after spinal cord injury with a fabric-based soft robotic glove. *Journal of Neuroengineering and Rehabilitation*, **15**, 1–10. https://doi.org/10.1186/s12984-018-0391-x

Dragusanu M, **Troisi D**, **Suthar B**, **Hussain I**, **Prattichizzo Dand Malvezzi M** (2024) Mglove-ts: A modular soft glove based on twisted string actuators and flexible structures. *Mechatronics*, **98**, 103141. https://doi.org/10.1016/j.mechatronics.2024.103141

EnableMe. (2015) Hand of hope.

Flores P, et al. (2011) A parametric study on the baumgarte stabilization method for forward dynamics of constrained multibody systems. *Journal of Computational and Nonlinear Dynamics*, 011019.

Gasser B, et al. (2017) Design and preliminary assessment of vanderbilt hand exoskeleton. *IEEE International Conference on Rehabilitation Robotics (ICORR), London, UK*, pp. 1537–1542. https://doi.org/10.1109/ICORR.2017.8009466

Haghshenas–Jarvani RM, et al. (2020) A pilot study on the design and validation of a hybrid exoskeleton robotic device for hand rehabilitation. *Journal of Hand Therapy*, **33**(2), 198–208. https://doi.org/10.1016/j.jht.2020.03.024

Haizman M (2007) Application of stabilization techniques in the dynamic analysis of multibody systems. *Applied and Computational Mechanics.*

Johnson G, et al. (2001) The design of a five–degree–of–freedom powered orthosis for the upper limb. *Journal of Engineering in Medicine*, **215**(3), 275–284. https://doi.org/10.1243/0954411011535867

Kladovasilakis N, et al. (2022) A novel soft robotic exoskeleton system for hand rehabilitation and assistance purposes. *Applied Sciences* **13**(1), 553. https://doi.org/10.3390/app13010553

Kovelman, H (2021). Executive summary, Myomo, Boston, MA, https://myomo.com/wp-content/uploads/2021/04/Executive-Summary.WS_.v03.April2021.pdf.

Lai J, **Song A**, **Wang J**, **Lu Y**, **Wu T.**, **Li H**, **Xu B,and Wei X** (2024) A novel soft glove utilizing honeycomb pneumatic actuators (hpas) for assisting activities of daily living. *IEEE Transactions on Neural Systems and Rehabilitation Engineering* **5**(3), 730–740. https://doi.org/10.1109/TNSRE.2023.3302612

Ledoux E, **Kumar N and Barth E** (2023) Orth *ohand extend: Design, modeling and evaluation* of a simple wrist-hand stretching orthosis for neurologically impaired patients. *TechRxiv Preprint*. https://doi.org/10.36227/techrxiv.170327839.98374610/v1

Li F, et al. (2023) Soft robotic glove with sensing and force feedback for rehabilitation in virtual reality. *Biomimetics* **8**(5), 425. https://doi.org/10.3390/biomimetics8010083

Polygerinos P, et al. (2014) Soft robotic glove for *combined* assistance and at-home rehabilitation. *Robotics and Autonomous Systems* **73**, 135–143. https://doi.org/10.1016/j.robot.2014.08.014

Rahman T, et al. (2000) A body–powered functional upper limb orthosis. *Journal of Rehabilitation Research and Development* **37**(6), 675–680.

Rehab F and Tran A (2022) Exercises 1 and 2. *Helpful Hand Exercises for Stroke Patients of All Ability Levels.*

Rucker C, et al. (2022) Task-space control of continuum robots using underactuated discrete rod models. *IEEE/RSJ International Conference on Intelligent Robots and Systems*. https://doi.org/10.1109/IROS47612.2022.9982271

Saebo. (2023a) Saeboflex product manual. https://zaorehab.com/wp-content/uploads/2022/12/product-manual-saeboflex_compressed.pdf

Saebo. (2023b) Saeboglove hand therapy rehabilitation glove. https://www.saebo.com/products/saeboglove?

Saharan L, et al. (2017) Igrab: Hand orthosis powered by twisted and coiled polymer muscles. *Smart Materials and Sensors* **26**(10), 105048. https://doi.org/10.1088/1361-665X/aa8929

Saldarriaga A, **Gutierrez-Velasquez E**, & **Colorado H** (2024) Soft hand exoskeletons for rehabilitation: Approaches to design, manufacturing methods, and future prospects. *Robotics* **13**(3), 50. https://doi.org/10.3390/robotics13030050

Shi XQ, et al. (2021) Effects of a soft robotic hand for hand rehabilitation in chronic stroke survivors. *Journal of Stroke and Cerebrovascular Diseases* **30**(7), 105812. https://doi.org/10.1016/j.jstrokecerebrovasdis.2021.105812

Sunnerhagen K, **Opheim A**, & **Murphy MA** (2019) Onset, time course and prediction of spasticity after stroke or traumatic brain injury. *Annals of Physical and Rehabilitation Medicine* **62**(6), 431–434. https://doi.org/10.1016/j.rehab.2018.04.004

Tang D, **Lv X**, **Zhang Y**, **Qi L**, **Shen C**, & **Shen W** (2024) A review on soft exoskeletons for hand rehabilitation. *Recent Patents on Engineering* **18**(4), 52–73. https://doi.org/10.2174/1872212118666230525145443

Tran P, et al. (2022). Flexotendon glove–iii: Voice–controlled soft robotic hand exoskeleton with novel fabrication method and admittance grasping control. *IEEE/ASME Transactions on Mechatronics* **27**(5), 3920–3931. https://doi.org/10.1109/TMECH.2022.3148032

https://doi.org/10.1017/wtc.2024.22 Published online by Cambridge University Press

Ueki S, et al. (2010). Development of a hand–assist robot with multi–degrees-of-freedom for rehabilitation therapy. *IEEE/ASME Transactions on Mechatronics* **17**(1), 136–146. https://doi.org/10.1109/TMECH.2010.2090353

World Stroke Organization. (2022). Global Fact Sheet 2022.

Yap HK, et al. (2017a). Design and preliminary feasibility study of a soft robotic glove for hand function assistance in stroke survivors. *Frontiers in Neuroscience* **11**, 547. https://doi.org/10.3389/fnins.2017.00547

Yap HK, et al. (2017b). A fully fabric-based bidirectional soft robotic glove for assistance and rehabilitation of hand impaired patients. *IEEE Robotics and Automation Letters* **2**(3), 1383–1390. https://doi.org/10.1109/LRA.2017.2669366

Yurkewich A, et al. (2020). Hand extension robot orthosis (hero) grip glove: Enabling independence amongst persons with severe hand impairments after stroke. *Journal of Neuroengineering and Rehabilitation* **17**(1), 33. https://doi.org/10.1186/s12984-020-00659-5

Zhao H, et al. (2016). A helping hand: Soft orthosis with integrated optical strain sensors and emg control. *IEEE Robotics and Automation Magazine* **23**(3), 55–64. https://doi.org/10.1109/MRA.2016.2582216

Cite this article: Ledoux ED, Kumar NS and Barth EJ (2024) Design, modeling, and preliminary evaluation of a simple wrist-hand stretching orthosis for neurologically impaired patients. *Wearable Technologies*, 5, e19. doi:https://doi.org/10.1017/wtc.2024.22